16TH EUROPEAN CONFERENCE ON EARTHQUAKE ENGINEERING THESSALONIKI 18 - 21 JUNE 2018

THE COMPARISON OF DIFFERENT FRAGILITY CURVE GENERATION TECHNIQUES TO ESTIMATE OBSERVED DAMAGE DISTRIBUTIONS

Shaghayegh KARIMZADEH[1], Koray KADAS[2], Aysegul ASKAN[3], Murat Altug ERBERIK[4], Ahmet YAKUT[5]

ABSTRACT

In a recent study by the authors, the suitability of using regionally derived simulated ground motion records in the development of fragility curves for local masonry structures of Erzincan, Turkey has been previously evaluated. It was concluded that simulated records could be alternatively used in order to derive regional fragility curves when there is a limited number of ground motion records at high intensity levels or in regions of sparse seismic networks. It was also observed that the use of alternative fragility curve generation methods and different ground motion sets (either real or simulated) could lead to significant differences in fragility values (i.e., exceedance probability) which would affect corresponding seismic damage estimations. This study introduces a novel procedure to further evaluate the efficiency of the alternative techniques by comparing the 'estimated' damage levels with the 'observed' states during the 1992 Erzincan (M_w=6.6) earthquake. For this purpose, the residential districts with masonry structures as the dominant structural type are examined. The Peak Ground Acceleration (PGA) values at the building locations are determined from the 'already verified' stochastic finite fault methodology. Utilizing the fragility curves developed with alternative methods by the authors, mean damage ratios for the regions examined are calculated. The results are compared with the 'observed' damage conditions of the masonry buildings examined and the performance of each method is evaluated quantitatively.

Keywords: Fragility Analysis; Masonry structures; Real ground motion records; Simulated ground motion records, Erzincan (Turkey)

1. INTRODUCTION

In order to provide reliable information for decision makers regarding the outcomes of potential earthquakes, seismic risk analysis should be performed accurately. One of the main steps in seismic risk analysis is vulnerability assessment performed through fragility functions. Regional characteristics of the ground motion set have a large impact on the generated fragility curves. Despite the efforts for dense seismic networks all over the world, there are still areas located in seismically active regions with sparsely-distributed or no seismic stations. In addition, even regions that are continuously monitored may lack records from some potential large earthquakes with long return periods. For such regions, a full range of recorded ground motions compatible with the regional seismicity may not be available. As an alternative, simulated ground motions can significantly expand the understanding of potential earthquakes and help to mitigate their outcomes on built environment. So far, most of the fragility curves in the literature have been derived based on global ground motion databases with records from different parts of the world (e.g.: Ansal et al. 2009, Ugurhan et al. 2011, Sørensen and Lang 2015, Gokkaya 2016). Simulated motions, on the other hand, have been employed in time history analyses of building structures (e.g.: Atkinson and Goda 2010, Atkinson et al. 2011, Galasso et al. 2012, Karimzadeh et al. 2017a, 2017b), yet not used in fragility derivations directly. The main purpose of this study is to assess

[1]Instructor, Civil Engineering Department, Middle East Technical University, Ankara, Turkey, shaghkn@metu.edu.tr
[2]Graduate Student, Civil Engineering Department, Middle East Technical University, Ankara, Turkey, kkadas@gmail.com
[3]Professor, Civil Engineering Department, Middle East Technical University, Ankara, Turkey, aaskan@metu.edu.tr
[4]Professor, Civil Engineering Department, Middle East Technical University, Ankara, Turkey, altug@metu.edu.tr
[5]Professor, Civil Engineering Department, Middle East Technical University, Ankara, Turkey, ayakut@metu.edu.tr

fragility curves which were obtained in a previous study (Karimzadeh et al. 2017d) for local building stock within a specified area utilizing regionally 'simulated' ground motion datasets with two main objectives: The first one is to compare these fragilities with the curves derived using global 'real' records. The other objective is to evaluate the sensitivity of these curves to alternative fragility curve generation methodologies. The simulated records which reflect regional seismicity in the study area, were obtained using stochastic finite-fault ground motion simulation methodology as introduced in Motazedian and Atkinson (2005). A set of scenario events is generated using the regional source, path and site models in the region of interest. The real records are selected based on global ground motion databases that involve earthquakes from different parts of the world.

In this study, fragility analyses are performed only for masonry building stock which account for the majority of the existing structures in Erzincan (http://www.tuik.gov.tr/Web2013/iletisim/iletisim.html). The previous studies have revealed that Peak Ground Acceleration (PGA) correlates well with inelastic response of masonry structures (Erberik 2008). Thus, fragility curves derived with respect to PGA (as intensity measure of seismic loading) are compared in sensitivity analyses. The local building dataset used in the analyses are collected from a walk-down survey in the study area (Askan et al. 2015a, Karimzadeh 2016). Finally, in this study loss estimation of a real earthquake in the selected area is performed and results are compared against the observations.

2. STUDY AREA

The region of interest is selected to be Erzincan which is located on eastern segments of North Anatolian Fault Zone (NAFZ). NAFZ is an active right-lateral strike-slip fault zone that lies in Northern Turkey and is one of the most active fault zones in the world. In the last century, NAFZ led to many destructive events in Turkey such as the 1939 Erzincan (Ms~8.0) event in the eastern part (Figure 1.a) and the 1999 Kocaeli (Mw=7.4) and 1999 Duzce (Mw=7.2) earthquakes in the western part close to Istanbul. Despite the critical seismic activity, Erzincan area in Eastern Turkey is not as much studied as the western sections of NAFZ. However, it is essential to study this region since Erzincan is one of the most hazardous cities in Eastern Turkey located on a deep alluvial basin within a tectonically complicated area, at the conjunction of three strike-slip faults: the right lateral North Anatolian Fault, the left lateral North East Anatolian Fault (NEAF), and the left lateral Ovacik fault (Figure 1.b). Historical records demonstrate around twenty large earthquakes in the proximity of Erzincan during the past 1000 years (Barka 1993). In addition to the 1939 event, Erzincan suffered from another destructive earthquake in 1992 (Mw=6.6) that led to significant structural damage as well as mortalities. However, the city center has a relatively sparse ground motion network despite the seismic activity. The other concern in this region is that majority of the existing structures in Erzincan (almost 60%) are vulnerable unreinforced masonry building types (http://www.tuik.gov.tr/Web2013/iletisim/iletisim.html). Since, the city center constitutes a region with high seismicity and few real records along with vulnerable masonry building stock, Erzincan is an ideal location for the case study presented herein.

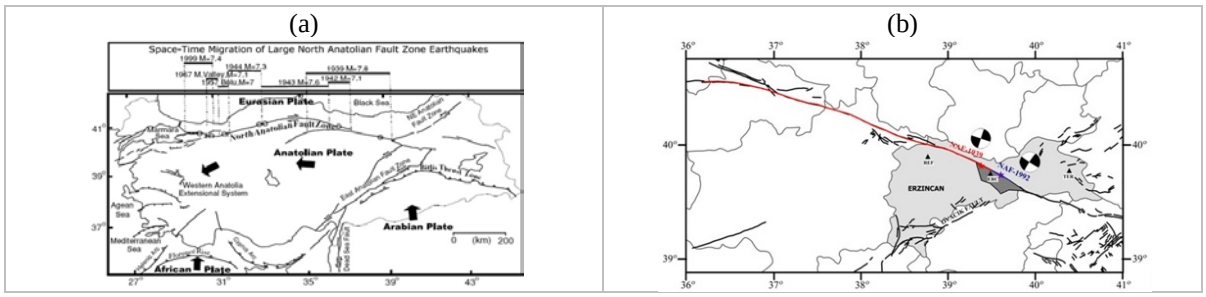

Figure 1. (a) Major tectonic structures around the Anatolian plate and large earthquakes that occurred on the NAFZ in the last century (b) Seismotectonics in the Erzincan region with the fault systems and the epicenters of the 1939 and 1992 events. (Figures 1.a and 1.b are adapted from Akyuz et al. (2002) and Askan et al. (2013), respectively).

3. SIMULATED AND REAL GROUND MOTION DATASETS

Seismic loss assessment in any region requires a suitable ground motion dataset compatible with the regional seismicity. In this study, to investigate the effect of input hazard in the final fragility curves and estimated losses, two alternative ground motion record sets are considered: Simulated and real records. To provide region-specific simulated ground motion dataset in the study area, simulations are performed along eastern segments of NAFZ.

In this study, for ground motion simulation the stochastic finite-fault technique based on a dynamic corner frequency approach as introduced by Motazedian and Atkinson (2005) is used. EXSIM software is employed for this method where the simulated rupture plane is divided into a number of small sub-faults, each of which is modelled as a stochastic point-source with an ω^{-2} spectrum (Hartzell 1978). To estimate the ground-shaking from the full rupture plane, the total contribution resulting from each sub-fault is summed at an observation point considering appropriate time delays. The following formula presents the acceleration spectrum of the ij^{th} subfault in terms of source, path and site effects:

$$A_{ij}(f) = CM_{0ij}H_{ij}\left[(2\pi f)^2/[1+\left(\frac{f}{f_{c_{ij}}}\right)^2]\right]e^{-\frac{\pi f R_{ij}}{Q(f)\beta}}G(R_{ij})A(f)e^{-\pi\kappa f} \quad (1)$$

where $C = \frac{\Re^{\theta\varphi}\cdot\sqrt{2}}{4\pi\rho\beta^3}$ is a scaling factor, $\Re^{\theta\varphi}$ is the radiation pattern, ρ is the density, β is the shear-wave velocity, $M_{0_{ij}} = \frac{M_0 S_{ij}}{\sum_{k=1}^{nl}\sum_{l=1}^{nw} S_{kl}}$ is the seismic moment, S_{ij} is the relative slip weight and $f_{c_{ij}}(t)$ is the dynamic corner frequency of the ij^{th} subfault where $f_{ij}(t) = N_R(t)^{-1/3}4.9\times10^6\beta\left(\frac{\Delta\sigma}{M_{0_{ave}}}\right)^{1/3}$. Here $\Delta\sigma$ is the stress drop, $N_R(t)$ is the cumulative number of ruptured subfaults at time *t*, and $M_{0_{ave}} = M_0/N$ is the average seismic moment of subfaults. R_{ij} is the distance from the observation point, $Q(f)$ is the quality factor, $G(R_{ij})$ is the geometric spreading factor, $A(f)$ is the site amplification term, and $e^{-\pi\kappa f}$ is a high-cut filter included to provide the spectral decay at high frequencies described with the Kappa factor of soils (Anderson and Hough 1984). H_{ij} is a scaling factor introduced to conserve the high-frequency spectral level of the sub-faults.

Ground motion simulations are performed for different scenario earthquakes with Mw=5.0, 5.5, 6.0, 6.5, 7.0, and 7.5 as well as the 1992 Erzincan event (Mw=6.6). For simulation of each scenario event, a total of 123 nodes inside of a rectangular region bounded by 39.45°-39.54° Eastern longitudes, 39.70°-39.78° Northern latitudes are considered. The spacing for nodes is approximately 1 km. Detailed shear wave velocity soil profiles are available at only nine nodes (Askan et al. 2015b). It is known that local soil conditions have a significant effect in the ground motion amplitudes on the corresponding soil surface. At nodes without detailed soil information, Vs30 value at the closest station is assigned. The final error by these sort of assumptions is believed to be negligible since the distance in between the nodes are short enough. For simulation of the 1992 Erzincan earthquake, the source, path, and site parameters are adapted from a previous study by Askan et al. (2013) where validations were performed. In this study, these parameters are adapted and modified whenever necessary for different scenarios according to the magnitude of each event. Table 1 provides information corresponding to the input parameters used for ground motion simulation of the scenarios. Simulations provide a total of 861 time histories including different soil conditions, source-to-site distance and magnitude values. Further details of the simulations can be found in Askan et al. (2013, 2015b, 2017).

To perform fragility analyses, out of 861 available records, a database of 200 time histories with a maximum PGA of 1g is selected. It is noted that the selected time histories are generated on a strike-slip fault mechanism covering a broad range of magnitudes (Mw=5.0-7.5) and the closest distance to the fault plane varies between 0.26 to 17.55 kilometers. The selected ground motion set is subdivided into 20 intensity levels with intervals of ΔPGA=0.05g so that an even distribution for structural responses can be obtained.

In addition to the simulated record set generated for the study, a set of real records seismologically compatible with the study area is formed. From the NGA-West2 database of Pacific Earthquake Engineering Research Center, 184 records are chosen with following seismological characteristics; fault type as strike-slip, magnitude range as 5.0-7.5, Joyner-Boore distance range as 0-20 km and $V_{s,30}$ range as 220-500 m/s (Ancheta et al. 2013). Out of these 184 available records, 113 records are randomly selected as the original records. Some selected records are linearly scaled in the time domain to obtain 10 records at each intensity level yielding 200 real records in total with a PGA range of 0.05-1g for the fragility analyses.

The records in both simulated and real datasets are baseline corrected and filtered with a 4th-order bandpass Butterworth filter (within f=0.25-25 Hz). Then PGA, Peak Ground Velocity (PGV), Housner intensity (HI), Arias intensity (I_a) are calculated. Figure 2 compares the distribution of mentioned ground motion parameters for both real and simulated record sets. The results demonstrate that even for a specified PGA, regional variability in selection process is taken into account. It is also observed that in terms of PGV, HI and I_a, a close match is obtained between the simulated and real sets. This observation is also promising in terms of using simulated motions in earthquake engineering practice.

Table 1. Simulation parameters used in the simulation of scenario earthquakes.

Parameter	**Value**
Hypocenter Location	39°42.3 N, 39°35.2 E
Hypocenter Depth	Variable
Depth to the Top of the Fault Plane	Variable
Fault Orientation	Strike: 125°, Dip: 90°
Fault Dimensions	Wells and Coppersmith (1994)
Crustal Shear Wave Velocity	3700 m/s
Rupture Velocity	3000 m/s
Crustal Density	2800 kg/m^3
Stress Drop	Mohammadioun and Serva (2001)
Quality Factor	$Q = 122 f^{0.68}$
Geometrical Spreading	$R^{-1.1}, \quad R \le 25\ km$ $R^{-0.5}, \quad R > 25\ km$
Duration Model	$T = T_0 + 0.05R$
Windowing Function	Saragoni-Hart
Kappa Factor	Regional kappa model (k_0=0.066: Askan et al. 2013)
Site Amplification Factors	Local soil model (Askan et al. 2015b)

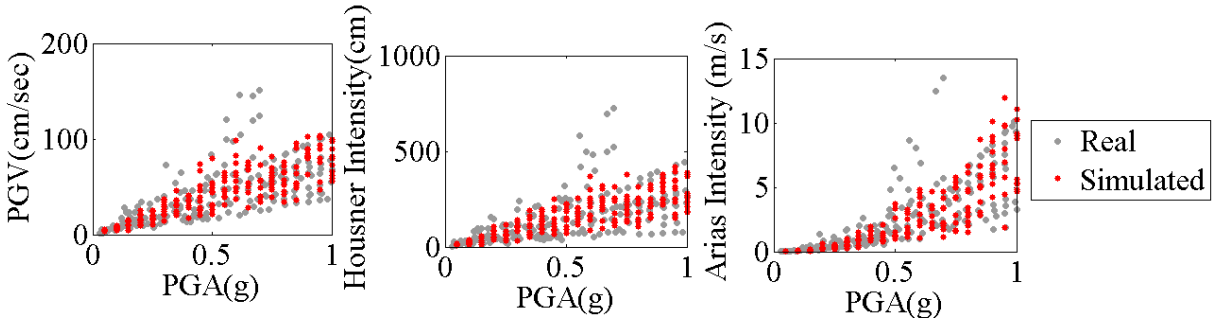

Figure 2. Distribution of the ground motion parameters for the selected real and simulated records

4. MASONRY BUILDING DATABASE USED IN THIS STUDY

Within a regional seismic loss assessment study, a detailed and realistic building inventory database is necessary. In this study, a walk-down survey in Erzincan is conducted where all masonry structures are classified into 9 sub-classes. Buildings within each sub-class are believed to exhibit, on average, similar damage behavior under identical seismic intensities. During this classification, two main structural parameters are considered: Number of stories (1-2-3 story) and level of compliance with the seismic design and construction principles (high: A, moderate: B and low: C). In definition of the abbreviated names for all sub-classes, 'MU' corresponds to masonry type, the number in the next digit denotes the number of stories, and the letter in the last digit indicates the level of compliance with seismic design codes and construction principles. For instance, MU2A corresponds to 2-story masonry building class with high level of compliance with seismic design codes. For estimation of dynamic response of structures under severe earthquakes, performing elastic analyses in general is believed not to be adequately conservative for assessing the complexity of precise failure patterns. In comparison, time history analysis is supposed to be more accurate in predicting the dynamic responses. For this purpose, in this study to assess the dynamic responses of the masonry classes Non-Linear Time History Analysis (NLTHA) within OpenSees platform is preferred (http://opensees.berkeley.edu). When dynamic responses of a large population of structures subjected to ground shakings are of concern, simplified and idealized structural models are preferred instead of complicated Multi-Degree-of-Freedom (MDOF) models. Accordingly, in this study, each building sub-class is idealized into an Equivalent Single-Degree-of-Freedom (ESDOF) system. To assess accurate dynamic responses of ESDOF models through NLTHA, it is important to consider a robust hysteresis model so that the inherent cyclic characteristics of each building sub-class subjected to ground shakings can be simulated. Among various hysteresis models available in the literature (e.g.: Park et al. 1987, Sucuoglu and Erberik 2004), for each ESDOF model, a well-known hysteresis model proposed by Ibarra et al. (2005) named as "Modified Ibarra-Medina-Krawinkler Deterioration Model with peak-oriented hysteretic response" is used.

Correspondingly, three fundamental structural parameters including period (T), strength ratio (η) and ductility factor (μ) are defined for all building sub-classes. In this study, for each subclass a total of 20 samples are simulated using Latin Hypercube Sampling technique (Olsson et al. 2003). Structural parameters corresponding to the simulated buildings can be found in Karimzadeh (2016) and Karimzadeh et al. (2017c, 2017d).

5. FRAGILITY ANALYSES

In this study, three structural performance levels are considered: Immediate Occupancy (IO: LS1), Life Safety (LS: LS2) and Collapse Prevention (CP: LS3). For generation of all sets of fragility curves, limit states corresponding to these performance levels are taken from Karimzadeh et al. (2017c, 2017d). In this section, first, two alternative ground motion data sets (the first set is the regionally-simulated and the second set is global real records) are employed to study the difference of the generated fragility curves to seismic hazard. Records are selected with respect to a total of 20 intensity levels with intervals of ΔPGA=0.05g. For each group of records (either real or simulated), at each intensity level, 10 records with different soil conditions, distance and magnitude values are selected. Therefore, there is a total of 200 records over the all intensity levels inside of each group of records.

In the second part, the sensitivity of the fragility analysis is investigated for two alternative fragility curve generation techniques using different probability exceedance functions. The first approach assumes a normal distribution function (ND-based) whereas the second approach performs frequency analysis (FA-based) to calculate the probabilities of exceedance. Equation 2 presents the formula used in the first approach whereas Equation 3 corresponds to the formula used for the second approach as follows:

$$P[D \geq LS_i | GMI_j] = a_A \quad (2)$$

$$P[D \geq LS_i | GMI_j] = \frac{n_A}{n_T} \quad (3)$$

where, a_A is the total area above the i^{th} limit state (LS_i), n_A is the sum of responses equal or above LS_i, and n_T stands for the total number of responses, both at the j^{th} ground motion intensity level (GMI_j). To obtain the final fragility curve, a cumulative lognormal distribution function is fitted to the scattered probabilities with least squares technique.

Comparison of the fragility curves for both real and simulated records using FA-based method has been presented in the previous study by the authors (Karimzadeh et al. 2017d). The results of that study revealed that for all limit states and subclasses except MU3C-LS3, the simulated records provide slightly higher exceedance probabilities than those of real records using FA-based method. In addition to the previously generated FA-based fragilities by Karimzadeh et al. (2017d), in the present study ND-based fragility curves are developed for both real and simulated records (Figure 3). The results demonstrate that for all subclasses and all limit states except collapse prevention (LS3), simulated records slightly provide higher damage levels for all ground motion intensities compared to those of real records. For collapse prevention limit state, fragility results from simulated records are below to those obtained using real records in lower ground motion intensities. However, after a certain ground motion intensity level simulated-record-based fragilities yield higher values compared to those obtained based on real records.

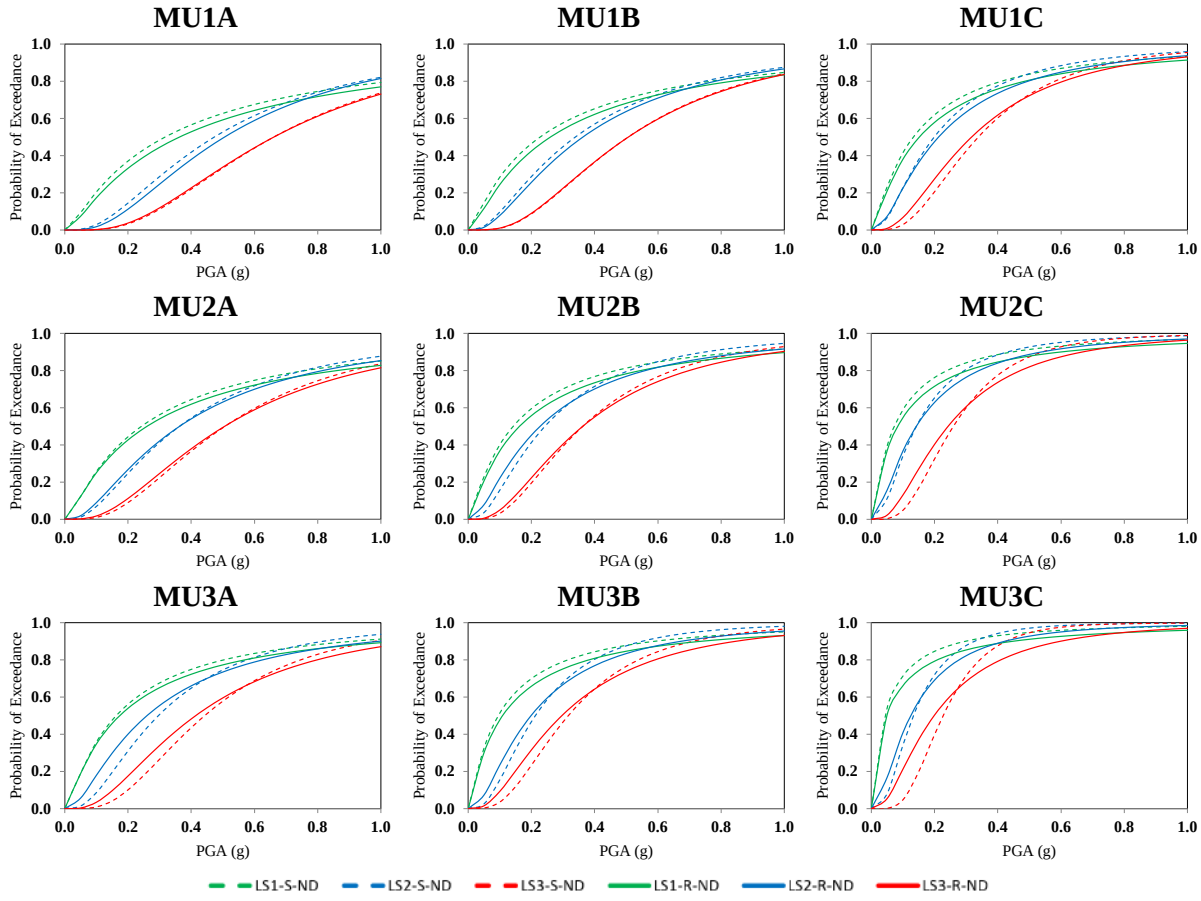

Figure 3. Comparison of fragility curves for Real versus Simulated Records using 200-record set and ND-based

When the FA-based and ND-based fragilities are compared for LS1, a negligible difference is observed between the results for all subclasses particularly when the curves are FA-based. This observation is much more pronounced for one-story buildings with higher building quality. However, when the results for LS2 and LS3 are of concern, the difference becomes noticeable especially for higher PGA levels. The maximum differences in terms of exceedance probabilities for ND-based and FA-based fragilities

reach up to 0.17 and 0.10, respectively. For both cases the simulated record-based fragility curves mostly yield higher values than those of real records. This may be attributed to the unpredictable nonlinear response of structures at higher intensity levels. Finally, comparison of the fragility curves obtained from simulated and real records yields a wide range of seismic responses for all masonry sub-classes. This is mostly because these are non-engineered structures without any standards regarding the material quality and the construction technique.

If the curves for all subclasses from two alternative methods using 200 simulated record set are compared, it can be observed that the exceedance probabilities calculated in according with ND-based method are greater than those of FA-based method (Figure 4). This difference is much more pronounced for strong and one-story masonry classes (e.g: MU1A). As the number of stories and the level of compliance with seismic design codes increases, the difference decreases. The maximum difference in terms of exceedance probability for all subclasses is approximately 0.35 for subclass MU1A and MU1C. Therefore, it is necessary to compare and validate the efficiency of fragility curves based on the two alternative assumptions for the probability of exceedance.

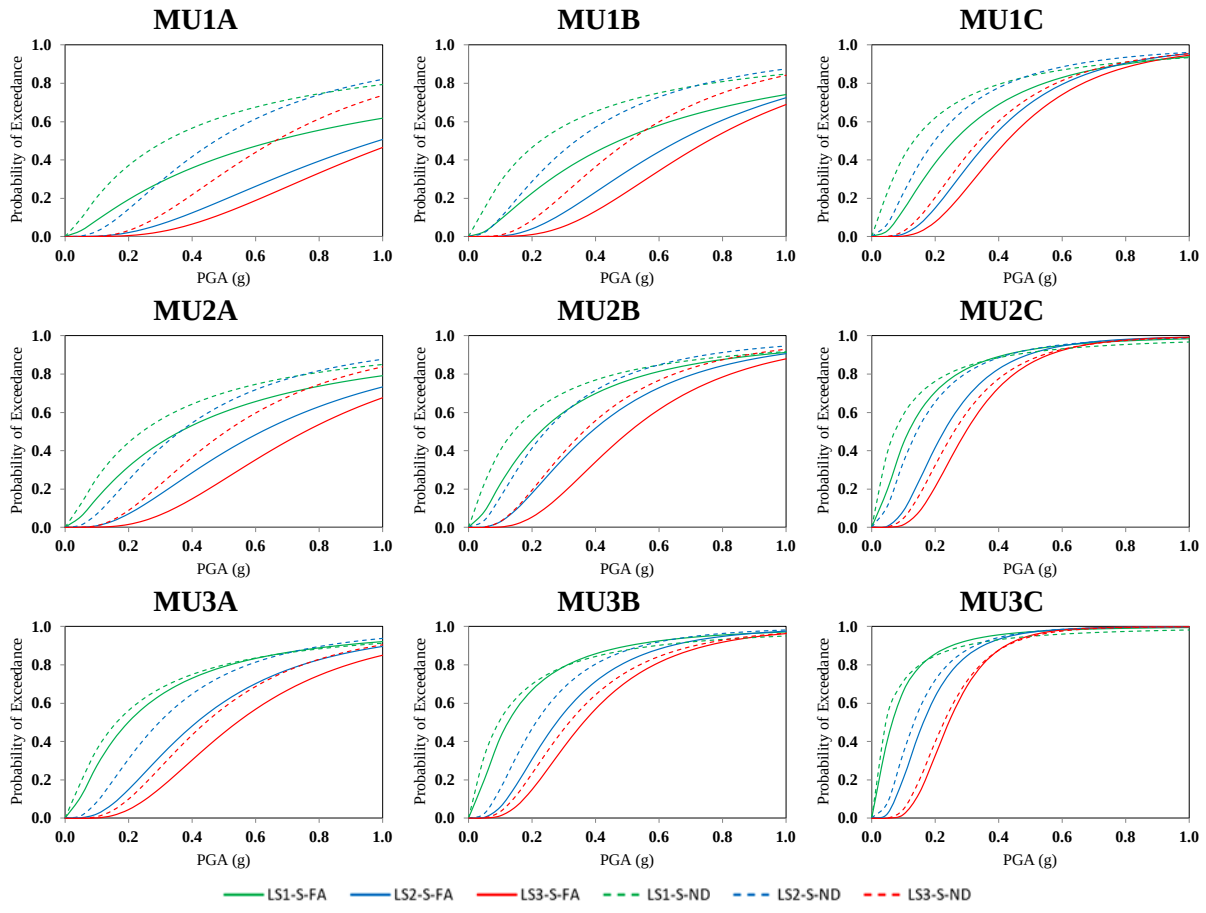

Figure 4. Comparison of fragility curves with respect to FA-based versus ND-based method using simulated 200- record set

6. VALIDATION OF THE GENERATED FRAGILITY CURVES BASED ON SEISMIC DAMAGE ESTIMATION DURING THE 1992 ERZINCAN (MW=6.6) EARTHQUAKE

The objective of this section is to validate the generated fragility curves for masonry building stock. For this purpose, seismic damage is estimated for the 1992 Erzincan (Mw=6.6) earthquake using the alternative fragility data presented previously. In order to investigate the effect of alternative datasets and approaches for fragility computations, estimated damage values are compared against the observed

ones during the 1992 (Mw=6.6) Erzincan earthquake. In this study, since the fragility curves are obtained for masonry building stock, only the districts with higher density of masonry buildings (greater than 90% of total building types) are considered. For this purpose, a total of four residential districts in Erzincan city with available building data are selected. Simulated records of the 1992 Erzincan (Mw=6.6) earthquake within the selected residential areas are compiled. Since fragility curves of masonry building stock are generated in terms of PGA, at the center of each district PGA is obtained from the simulated records. Percent distribution of the masonry buildings with respect to the number of stories and compliance level for the selected districts is achieved. Table 2 gives the latitudes, longitudes, simulated PGA and the percent distribution of the masonry building stock with respect to the number of stories as well as the code compliance in the selected districts. The information corresponding to the percent distribution of the buildings with respect to the number of stories and the level of compliance with seismic design codes in the selected residential areas are gathered from the walk-down survey in the study area (Karimzadeh 2016).

Table 2. Information corresponding to the selected districts in Erzincan region.

Name of District	**Lat. (º)**	**Long. (º)**	**Simulated PGA (g)**	**Code Compliance (%)**		**1-Story MU (%)**	**2-Story MU (%)**	**3-Story MU (%)**
				A	**B**			
Kizilay	39.7448	39.4897	0.6406	50	50	95	2	3
Aksemsettin	39.7506	39.5148	0.6374	-	100	90	8	2
Halitpasa	39.7440	39.4789	0.3698	50	50	65	25	10
Hocabey	39.7416	39.4849	0.4191	50	50	74	19	7

In this study, evaluation of seismic damage is performed through MDR which uses a single value to express the disaggregated damage estimates (as implemented by Askan and Yucemen 2010). To compute MDRs at the selected residential districts, firstly DPMs are formed as originally introduced by Whitman et al. (1997). Each row of DPM corresponds to a certain seismic damage state while each column of this matrix stands for a constant level of ground motion intensity level. Finally, each element of this matrix, denoted by P_k (DS, I), stands for the probability of experiencing a certain damage state (DS) when the considered structure is exposed to the ground motion intensity level of I. The definition is simply expressed as follows:

$$P_k(DS, I) = \frac{N(DS,I)}{N(I)} \tag{4}$$

where, N(I) is the number of k^{th}-type of buildings in the area subjected to a ground motion of intensity I and N(DS, I) is the number of structures in damage state (DS), among the N(I) buildings.

In the present study, a total of 4 damage states is considered for damage states: none (DS_1), light (DS_2), moderate (DS_3) and severe (DS_4). It is noted that for all damage states considered in this study the values proposed by Gurpinar et al. (1978) are considered. Then, DPMs for the selected districts are formed using the information provided by alternative fragility curves. Finally, to compute the MDRs at the selected residential districts, the following formula is used:

$$MDR(IL) = \sum_{DS} P_k(DS, IL).CDR(DS) \tag{5}$$

where, CDR(DS) represents the central damage ratio corresponding to damage state DS. IL stands for the ground motion intensity level which is PGA of a certain residential district in this study.

For estimation of MDRs at the selected residential districts with dense number of masonry building types, the results of four approaches are used. It is aimed herein to investigate the effect of using either real or simulated records along with two alternative fragility curve generation methods for damage

estimation. The first and second approaches both uses the fragility information obtained based on simulated ground motions with 200-record sets. The difference in between these approaches is that the first approach uses ND-based fragility curve derivation method to calculate the probability of exceedance while the second one is obtained by FA-based technique. The third approach is based on fragility information from real ground motions and ND-based technique. Finally, The MDRs from the fourth approach are based on fragility curves obtained using real records and FA-based technique. In this study, the MDRs obtained from the first, second, third and fourth approaches are named as $MDR_{S\text{-}ND\text{-}200}$, $MDR_{S\text{-}FA\text{-}200}$, $MDR_{R\text{-}ND\text{-}200}$, $MDR_{R\text{-}FA\text{-}200}$, respectively. In this study, the observed MDRs for the 1992 Erzincan earthquake are estimated from the previous studies in the field by Sucuoglu and Tokyay (1992), Sengezer (1993) and Erdik et al. (1994). Table 3 presents the observed damage levels during the 1992 Erzincan earthquake along with the estimated MDRs from the abovementioned four different approaches. The results reveal that for two districts, Halitpasa and Hocabey, the estimated PGA values are lower than those corresponding to Kizilay and Aksemsettin. As a result, the observed and estimated MDRs for the Halitpasa and Hocabey are less than the ones corresponding to the Kizilay and Aksemsettin. Overall, comparison of the observed and estimated damage levels for the 1992 Erzincan earthquake demonstrates that for the selected residential areas the results from all four approaches are in a good agreement while the accuracy of the second and fourth approaches (using FA-based fragilities) is higher than the accuracy of the first and third approaches (using NA-based fragilities). These differences may be attributed not only to the methodology used but also to existence of building types other than masonry (e.g.: reinforced concrete) in the selected districts as well as the subjectivity in assigning damage states for the buildings of each district in the field. The results in Table 3 also reveal that both real and simulated records provide the same levels of MDRs in the selected districts while using the same fragility generation technique (either FA-based or ND-based).

Table 3. Observed and estimated MDR values for the 1992 Erzincan earthquake.

District	**Observed MDR (%)**	**Estimated MDR (%)**			
		$MDR_{S\text{-}ND\text{-}200}$	**$MDR_{S\text{-}FA\text{-}200}$**	**$MDR_{R\text{-}ND\text{-}200}$**	**$MDR_{R\text{-}FA\text{-}200}$**
Kizilay	29.65	52.57	30.43	51.82	29.15
Aksemsettin	39.00	58.68	38.59	57.85	38.07
Halitpasa	13.54	33.60	16.22	33.29	14.60
Hocabey	13.83	37.32	18.31	36.72	16.71

Finally, to measure the goodness of match between the estimated damage values from different approaches and the observed damage levels, the Root Mean Square Error (RMSE) function is defined as follows:

$$RMSE = \left(\frac{1}{N}\sum_{i=1}^{N}(MDR(est)_i - MDR(obs)_i)^2\right)^{1/2} \quad (6)$$

where N is the number of residential districts with available real MDRs, which is equal to 4 herein, $MDR(est)_i$ and $MDR(obs)_i$ is the estimated and observed MDRs at i^{th} residential district, respectively. Also, the correlation coefficients in between the estimated (by implementing four different methods) and the observed MDRs are calculated. Table 4 summarizes the calculated correlation coefficients and the corresponding error values. Comparison of these values reveals that among the four approaches, the MDRs estimated using the second and fourth approaches ($MDR_{S\text{-}FA\text{-}200}$ and $MDR_{R\text{-}FA\text{-}200}$) have the maximum correlation with the observed MDRs with correlation coefficients of 0.9974 and 0.9972 respectively. For these two approaches with FA-based fragilities, the RMSEs are less than the approaches where normal distribution function is used for derivation of the fragility curves. Therefore, the assumption of frequency analysis for calculation of probabilities of exceedance in fragility curve generation methodology (Equation 3) yields more accurate estimation of observed damage levels. The results also reveal that fragility information derived from locally simulated ground motions using stochastic finite-fault methodology yields reliable damage distributions.

Table 4. Performance of different damage estimation approaches in predicting the observed MDRs during the 1992 Erzincan earthquake.

District	Error (RMSE)	Coefficient of correlation
$MDR_{S\text{-}ND\text{-}200}$	21.6017	0.9883
$MDR_{S\text{-}FA\text{-}200}$	2.6471	0.9974
$MDR_{R\text{-}ND\text{-}200}$	20.9824	0.9892
$MDR_{R\text{-}FA\text{-}200}$	1.6202	0.9972

7. CONCLUSIONS

The focus of this study is to investigate the sensitivity of fragility curves for masonry structures located in Erzincan, Turkey to alternative ground motion sets (i.e., simulated versus real). The other question of interest is to evaluate the effect of alternative fragility curve generation methods (i.e., FA-based versus ND-based) in the generated fragility curves. Then, to examine the suitability of different approaches for seismic loss assessment, seismic damage for the 1992 Erzincan (Turkey) event is estimated at districts with dense number of masonry building stock in Erzincan using different fragility information. Afterwards, the estimated damage levels from alternative approaches are compared against the observed values during the 1992 Erzincan (Turkey) earthquake. The following main conclusions can be derived from the numerical exercises presented in this study:

- When the results for alternative ground motion datasets (i.e., simulated versus real) are compared, it is observed that regardless of the fragility curve generation technique at all ground motion intensity levels, for all subclasses and all limit states except collapse prevention, simulated records slightly provide higher probabilities of exceedance compared to those of real records. This observation indicates that simulated records could be alternatively used in order to derive regional fragility curves when there is limited number of ground motion records at high intensity levels or in regions of sparse seismic networks. Correspondingly, reliable and conservative fragility curves could be obtained by introducing ground motion variability in terms of magnitude, source to site distances and soil conditions for a certain intensity level through the simulations. This conclusion is valid in the case of ground motion databases that consist of a large number of simulated records such as the presented study.

- Sensitivity analyses with respect to fragility curve generation technique reveals that there is significant difference in between FA-based and ND-based fragility curves particularly for strong and one-story masonry classes (e.g: MU1A). The effect of using either FA-based or ND-based technique becomes insignificant for weak masonry classes with the highest number of stories (e.g.: MU3C).

- Comparison of the estimated damage levels from the presented fragility curves against the observed damage data obtained after the 1992 Erzincan earthquake reveals that for both ground motion datasets (real and simulated records), the accuracy of FA-based fragilities are higher than the ND-based fragilities.

- Finally, comparison of the estimated damage levels for the 1992 Erzincan (Turkey) event shows that while using the same fragility curve generation technique (either ND-based or FA-based), the difference in between estimated damage levels from real and simulated records is negligible. This observation indicates that use of simulated ground motions is promising for seismic loss estimation studies in regions of sparse data or poor seismic networks.

The results of this study can be further evaluated in the future for the other seismically-active areas. In addition, the effect of alternative ground motion simulation techniques (such as deterministic and hybrid methods) on seismic loss estimation studies can be investigated.

8. ACKNOWLEDGMENTS

The data in this study has been collected with the financial support by a Turkish National Geodesy and Geophysics Union through the project with grant number TUJJB-UDP-01-12. The first author is partially funded by JICA-SATREPS through the MarDiM project entitled “Earthquake and Tsunami Disaster Mitigation in the Marmara Region and Disaster Education in Turkey”. The second author has been financially supported by The Scientific and Technological Research Council of Turkey (TUBITAK) through Domestic Doctoral Scholarship Program. All these supports are highly acknowledged.

9. REFERENCES

Akyuz HS, Hartleb R, Barka A, Altunel E, Sunal G, Meyer B, Armijo R (2002). Surface rupture and slip distribution of the 12 November 1999 Duzce earthquake (M 7.1), North Anatolian fault, Bolu, Turkey. *Bulletin of Seismological Society of America*, 92 (1): 61–66.

Ancheta TD, Darragh RB, Stewart JP, Seyhan E, Silva WJ, Chiou BSJ, Wooddell KE, Graves RW, Kottke AR, Boore DM, Kishida T, Donahue JL (2013). *PEER NGA-West2 Database*, Pacific Earthquake Engineering Research Center.

Anderson J, Hough S (1984). A model for the shape of the Fourier amplitude spectrum of acceleration at high frequencies. *Bulletin of Seismological Society of America*, 74 (5): 1969-1993.

Ansal A, Akinci A, Cultrera G, Erdik M, Pessina V, Tonuk G, Ameri G (2009). Loss estimation in Istanbul based on deterministic earthquake scenarios of the Marmara Sea region (Turkey). *Soil Dynamics and Earthquake Engineering*, 29: 699-709.

Askan A, Asten M, Erberik MA, Erkmen C, Karimzadeh S, Kilic N, Sisman FN, Yakut A (2015a). Seismic Damage Assessment of Erzincan, *Turkish National Union of Geodesy and Geophysics project*. Project no: TUJJB-UDP-01-12, Turkey, Ankara, (In Turkish).

Askan A, Karimzadeh S, Asten M, Kilic N, Şişman FN, Erkmen C (2015b). Assessment of seismic hazard in Erzincan (Turkey) region: construction of local velocity models and evaluation of potential ground motions. *Turkish Journal of Earth Science*, 24 (6): 529-565.

Askan A, Karimzadeh S, Bilal M (2017). Seismic intensity maps for North Anatolian Fault Zone (Turkey) based on recorded and simulated ground motion data. In: Ibrahim Cemen and Yucel Yilmaz (ed) Neotectonics and Earthquake Potential of the Eastern Mediterranean Region, *in Active Global Seismology: Neotectonics and Earthquake Potential of the Eastern Mediterranean Region*, John Wiley & Sons, Inc., Hoboken, NJ, USA.

Askan A, Sisman FN, Ugurhan B (2013). Stochastic strong ground motion simulations in sparsely-monitored regions: A validation and sensitivity study on the 13 March 1992 Erzincan (Turkey) earthquake. *Soil Dynamics and Earthquake Engineering*, 55: 170-181.

Askan A, Yucemen MS (2010). Probabilistic methods for the estimation of potential seismic damage: Application to reinforced concrete buildings in Turkey. *Structural Safety*, *32*(4): 262-271.

Atkinson GM, Goda K (2010). Inelastic seismic demand of observed versus simulated ground-motion records for Cascadia subduction earthquakes. *Bulletin of the Seismological Society of America*, 2010 (100): 102–15.

Atkinson GM, Goda K, Assatourians K (2011). Comparison of nonlinear structural responses for accelerograms simulated from the Stochastic Finite-Fault approach versus the Hybrid Broadband approach. *Bulletin of the Seismological Society of America***,** 2011 (101): 2967–80.

Barka A (1993). The tectonics of Erzincan basin and 13 March 1992 Erzincan earthquake, *Proceedings of the 2nd Turkish National Earthquake Engineering Conference*, Istanbul Technical University Structures and Earthquake Applications-Research Center, (in Turkish), pp 259-270.

Erberik MA (2008). Generation of fragility curves for Turkish masonry buildings considering in- plane failure modes. *Earthquake Engineering & Structural Dynamics*, 37 (3): 387-405.

Erdik M, Yuzugullu O, Karakoc C, Yilmaz C, Akkas N (1994). March 13, 1992 Erzincan (Turkey) earthquake, Earthquake Engineering, *Tenth World Conference*, Balkema, Rotterdam.

Galasso C, Zareian F, Iervolino I, Graves RW (2012). Elastic and post-elastic response of structures to Hybrid Broadband synthetic ground motions. *Proceedings of the 9th International Conference on Urban Earthquake Engineering/4th Asia Conference on Earthquake Engineering*, Tokyo Institute of Technology, Tokyo, Japan.

Gokkaya K (2016). Geographic analysis of earthquake damage in Turkey between 1900 and 2012. *Geomatics, Natural Hazards and Risk, 7* (6), 1948-1961.

Gurpinar A, Abali M, Yucemen M, Yesilcay Y (1978). Feasibility of obligatory earthquake insurance in Earthquake Engineering Research Center, Civil Engineering Department, METU, Turkey, Report 78-05.

Hartzell S (1978). Earthquake Aftershocks as Green's Functions. *Geophysical Research Letters*, 5 (1): 1-4.

Ibarra LF, Medina RA, Krawinkler H (2005). Hysteretic models that incorporate strength and stiffness deterioration. *Earthquake Engineering and Structural Dynamics*, 34 (12): 1489-511.

Karimzadeh (2016). Use of Simulated Strong Ground Motion Records in Earthquake, *Ph.D. Thesis*, Faculty of Civil Engineering, Middle East Technical University, Ankara, Turkey.

Karimzadeh S, Askan A, Yakut A, Ameri G (2017a). Assessment of Alternative Simulation Techniques in Nonlinear Time History Analyses of Multi-Story Frame Buildings: A Case Study. *Soil Dynamics and Earthquake Engineering*, 98: 38-53.

Karimzadeh S, Askan A, Yakut A (2017b). Assessment of simulated ground motions for their use in structural engineering practice; a case study for Duzce (Turkey). *Pure and Applied Geophysics*, 174 (9), 3325–3329.

Karimzadeh S, Askan A, Erberik MA, Yakut A (2017c). Seismic Damage Assessment in Erzincan (Turkey) utilizing Synthetic Ground Motion Records, 1*6th World Conference on Earthquake (16WCEE)*, Santiago, Chile, Paper No: 2309.

Karimzadeh S, Kadas K, Erberik MA, Askan A, Yakut A (2017d). A Study on Fragility Analyses of Masonry Buildings in Erzincan (Turkey) Utilizing Simulated and Real Ground Motion Records, *the 10th International Conference on Structural Dynamics (EURODYN)*, Rome, Italy, Vol: 199, pp 188–193, (2017). DOI: 10.1016/j.proeng.2017.09.237.

Mohammadioun B, Serva L (2001). Stress drop, slip type, earthquake magnitude, and seismic hazard. *Bulletin of Seismological Society of America*, 91 (4): 694-707.

Motazedian D, Atkinson GM (2005). Stochastic finite-fault modeling based on a dynamic corner frequency. *Bulletin of Seismological Society of America*, 95 (3): 995–1010.

Olsson A, Sandberg G, Dahlblom O (2003). On Latin hypercube sampling for structural reliability analysis. *Structural Safety*, 25 (1): 47-68.

OpenSees 2.4.5, Computer Software, University of California, Berkeley, CA. http://opensees.berkeley.edu. [Last Visited on September 2017].

Park YJ, Reinhorn AM, Kunnath SK (1987). IDARC: Inelastic Damage Analysis of Reinforced Concrete Frame –Shear all Structures, *Technical Report NCEER-87-0008*, State University of New York at Buffalo.

Sengezer BS (1993). The Damage Distribution during March 13, 1992 Erzincan Earthquake, proceedings, *2nd National Earthquake Engineering Conference*, pp 404-415.

Sørensen MB, Lang DH (2014). Incorporating Simulated Ground Motion in Seismic Risk Assessment-Application to the Lower Indian Himalayas. *Earthquake Spectra*, 31 (1): 71-95.

Sucuoglu H, Erberik MA (2004). Energy Based Hysteresis and Damage Models for Deteriorating Systems. *Earthquake Engineering and Structural Dynamics*, 33 (1): 69-88.

Sucuoglu H, Tokyay M (1992). 13 Mart 1992 Erzincan earthquake engineering report, civil engineering department, Ankara, pp 102.

TUIK, http://www.tuik.gov.tr/Web2013/iletisim/iletisim.html, [last visited on September 2017].

Ugurhan B, Askan A, Erberik MA (2011). A methodology for seismic loss estimation in urban regions based on ground-motion simulations. *Bulletin of the Seismological Society of America*, 101: 710–725.

Wells D, Coppersmith K (1994) New empirical relationships among magnitude, rupture length, rupture width, rupture area, and surface displacement. *Bulletin of Seismological Society of America*, 84 (4): 974-1002.

Whitman RV, Anagnos T, Kircher CA, Lagorio HJ, Lawson RS, Schneider P (1997). Development of a national earthquake loss estimation methodology. *Earthquake Spectra*, 13 (4): 643–661.